

CHAPTER 4

EXPERIMENTAL PROCEDURE

Experimental Apparatus for Measuring Pore Structure Through Pressure Measurement.

One main purpose of this study is to characterize the pore structure through two and three dimensional approaches.

1. Three-Dimensional Approach.

An experimental apparatus was constructed to characterize the pore structure in the three-dimensional condition by measuring the pressure drop of rarefied air flow across the porous ceramic sample using a castor oil manometer. A PVC tube of 0.025 m (ID) was used to allow rarefied air flow through a critical nozzle and the porous ceramic material. Ball valves were used to control the constant air flow rate supplied from a wet-test gas meter. This system was designed to measure the pressure drop under rarefied flow condition by using a vacuum pump to obtain a long mean free path of the gas molecule. The absolute pressure was measured with a mercury manometer attached to the castor oil manometer as illustrated in figure 4.1. A bypass connection was installed for the purpose of reducing the air flow through the porous ceramic specimen. In the experiment, mass flow rate of air was varied from 0.015 to 1.166 liter/min, which was kept constant by flowing air through critical nozzles of different nozzle diameters and at different absolute gas pressures. The observed pressure drop was thus varied from about a half atmosphere down to several ten torrs so as to obtain a longer mean free path of air molecules that became comparable to the mean pore size of the refractory. The readings of absolute pressure and pressure drop should be very accurate within ± 0.1 mm for both the mercury and castor oil manometers. Various specimens of different compositions and mean pore radii were experimented in order to study the effect of pore size on air flow rate and pressure drop per unit length of a specimen. Section 3.1(chapter 4) explained the material preparation of these specimens. The test specimens were of cylindrical shape, 0.05 m in diameter and of thickness between 0.003-0.009 m.

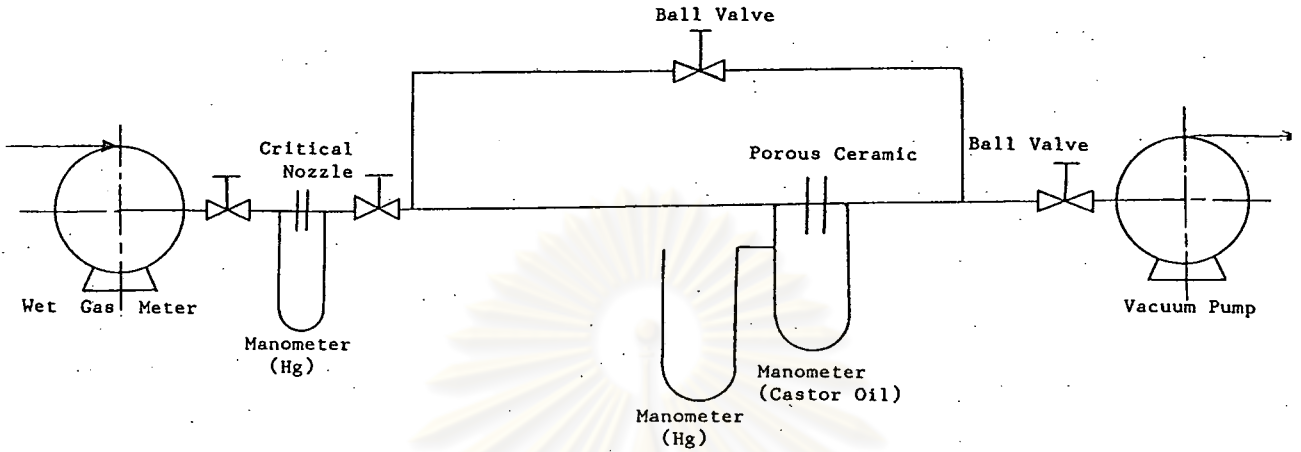


Figure 4.1 Diagram of Experimental Apparatus

2. Two-Dimensional Approach.

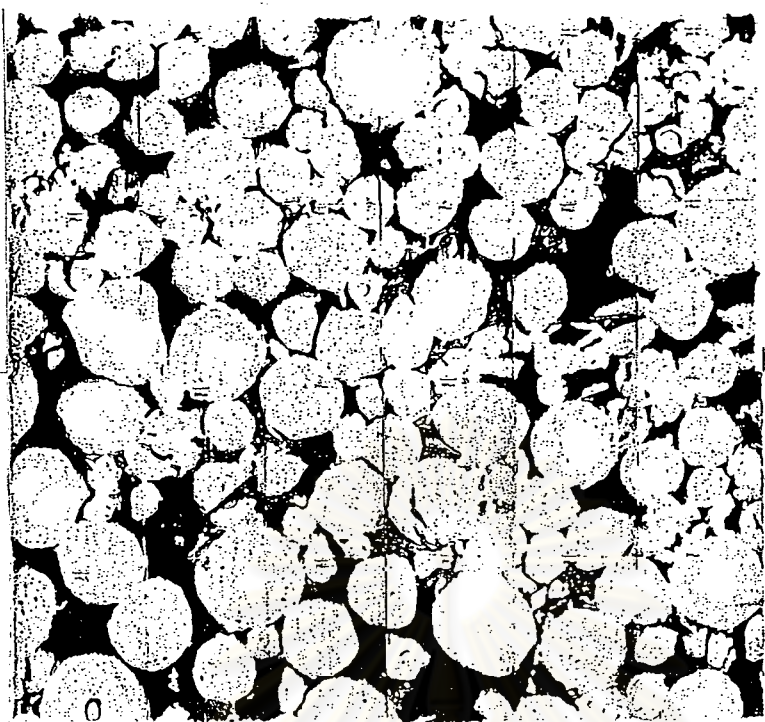
2.1 Reflecting Microscope.

A reflecting microscope was used to observe the micro-structure of the matrix and the interface between the matrix and the grain particles. Figures 4.2-4.4 illustrated the photomicrographs of specimens that are sliced into different thicknesses in order to show the three-dimensional homogeneity.

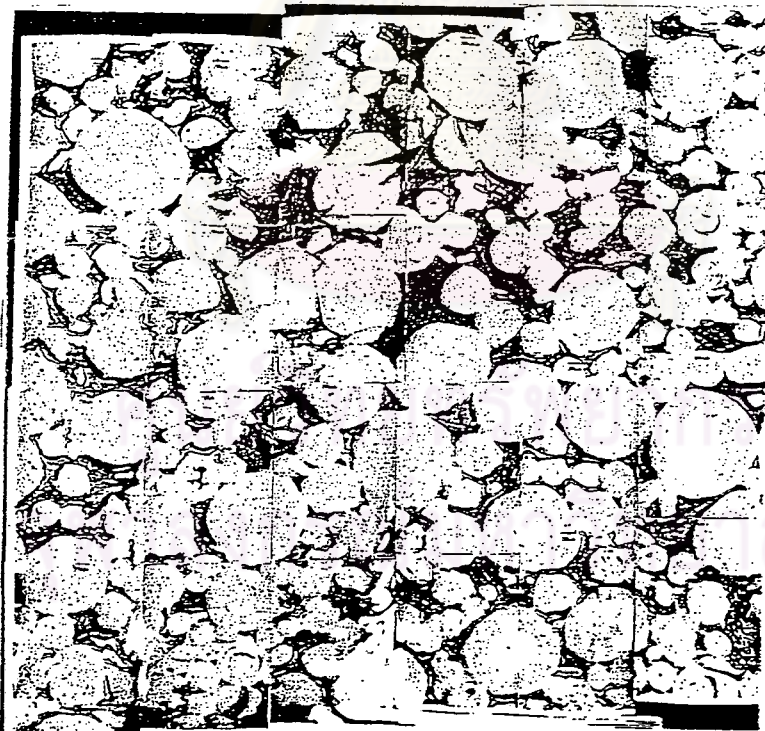
For pore structure in the test body to have a fractal nature, the following equation has to be satisfied:

$$N(r) = (\text{Similarity ratio})^{-D} \quad (4.1)$$

Here, the fractal dimension, D is defined in equation (4.2)

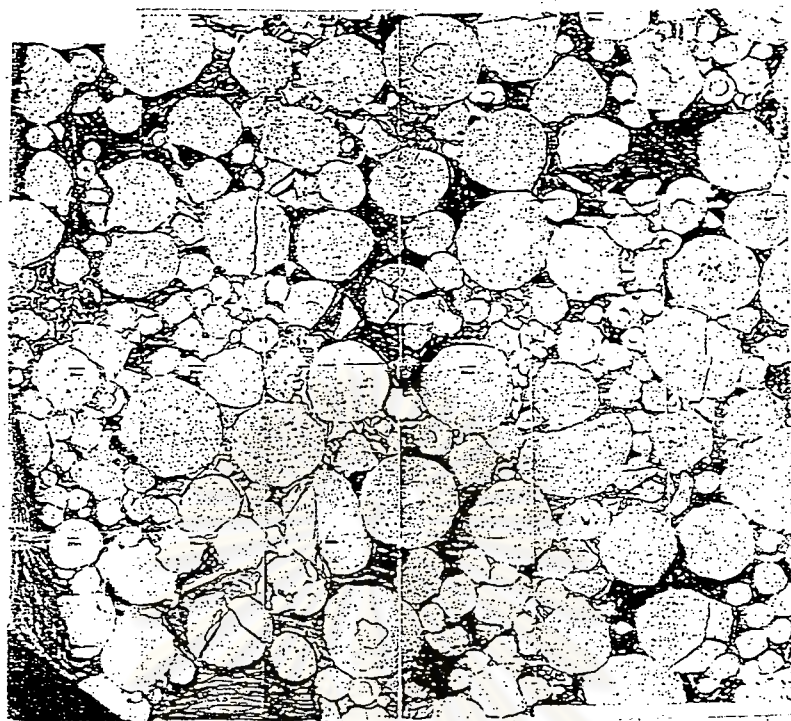


A

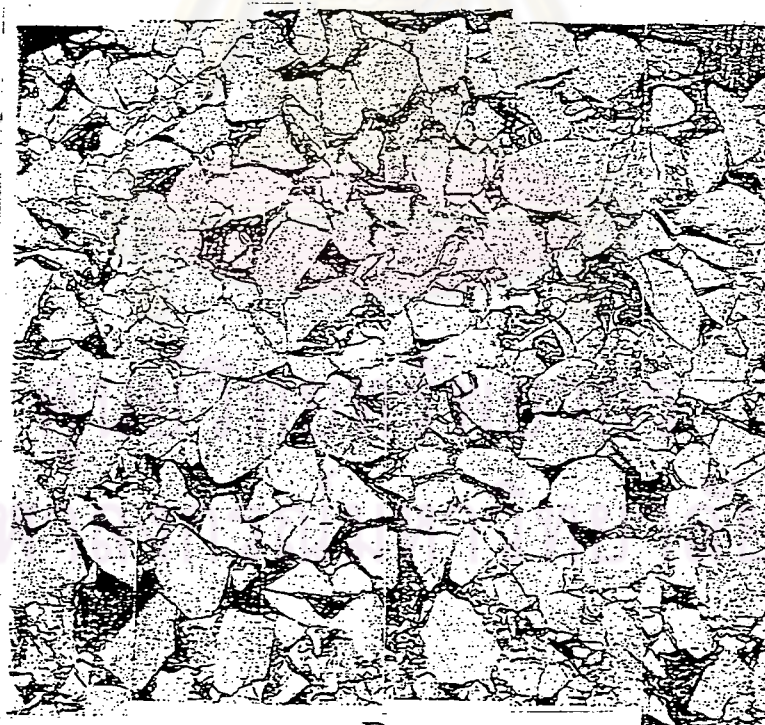


B

Figure 4.2 Photomicrographs of Specimens A and B

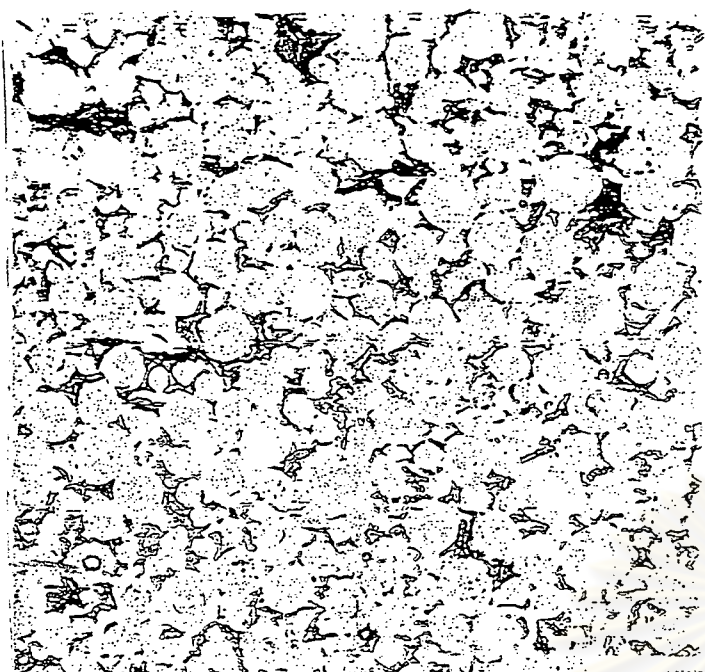


C



D

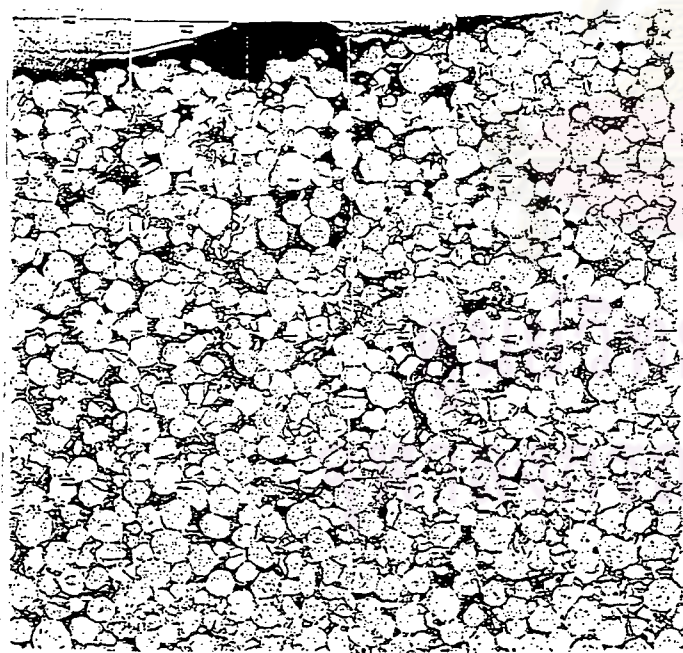
Figure 4.3 Photomicrographs of Specimens C and D



E



F



G

Figure 4.4 Photomicrographs of Specimens E, F and G

$$D = \frac{\log N(r)}{\log (1/r)} = -\frac{\log N(r)}{\log (r)} \quad (4.2)$$

$N(r)$ = number of subsections (square of side r) containing at least one small portion of any pore

r = representative scale of the similarity ratio

D = fractal dimension

The relationship between $N(r)$ and r , as read from the photomicrographs in figures 4.2-4.4, were plotted on log-log scale in figure 4.5 and summarize in table 4.1. Table 4.1 showed the number of subsections $N(r)$ required to cover all the pores. The fractal dimensions calculated from the slopes of the lines in figure 4.5 are also given in table 4.1 for these specimens.

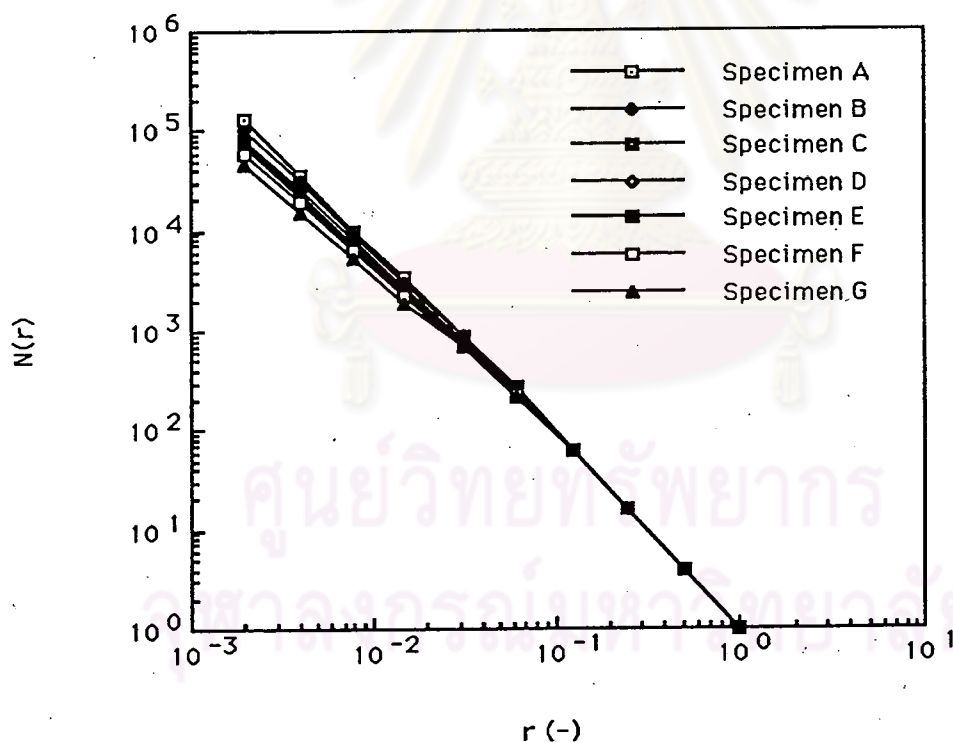


Figure 4.5 Number of Segments $N(r)$ Required to Cover the Pores vs. Similarity Ratio r

Table 4.1 Number of Segments $N(r)$ Required to Cover the Pores and the Fractal Dimensions of Each Specimen

Specimen	A	B	C	D	E	F	G
r	$N(r)$	$N(r)$	$N(r)$	$N(r)$	$N(r)$	$N(r)$	$N(r)$
1/512	1.3x 10^5	1.0x 10^5	8.2x 10^4	8.0x 10^4	7.0x 10^4	6.0x 10^4	4.7x 10^4
1/256	3.6x 10^4	3.1x 10^4	2.6x 10^4	2.3x 10^4	2.1x 10^4	1.9x 10^4	1.5x 10^4
1/128	1.0x 10^4	9.4x 10^3	8.0x 10^3	7.3x 10^3	6.8x 10^3	6.2x 10^3	5.2x 10^3
1/64	3.5x 10^3	3.0x 10^3	2.7x 10^3	2.5x 10^3	2.3x 10^3	2.2x 10^3	1.9x 10^3
1/32	9.0x 10^2	8.9x 10^2	7.9x 10^2	7.8x 10^2	7.4x 10^2	7.1x 10^2	6.8x 10^2
1/16	2.7x 10^2	2.6x 10^2	2.4x 10^2	2.3x 10^2	2.3x 10^2	2.2x 10^2	2.2x 10^2
1/8	6.4x 10^1	6.4x 10^1	6.4x 10^1	6.4x 10^1	6.4x 10^1	6.4x 10^1	6.4x 10^1
1/4	1.6x 10^1	1.6x 10^1	1.6x 10^1	1.6x 10^1	1.6x 10^1	1.6x 10^1	1.6x 10^1
1/2	4.0x 10^0	4.0x 10^0	4.0x 10^0	4.0x 10^0	4.0x 10^0	4.0x 10^0	4.0x 10^0
1	1.0x 10^0	1.0x 10^0	1.0x 10^0	1.0x 10^0	1.0x 10^0	1.0x 10^0	1.0x 10^0
Fractal Dimension	1.75	1.73	1.71	1.70	1.67	1.64	1.56

2.2 Image Analysis.

Image analyzer, model Luzex III, was used to measure pore geometry such as individual and total pore areas, frame area (total pore area and total granule area), their maximum and minimum values and standard deviation, as shown in table 4.2. Therefore, two-dimensional porosity can be obtained from image analysis of the photomicrographs.

Table 4.2 Two-Dimensional Porosity Obtained from Image Analysis

Specimen / Diameter	A	B	C	D	E	F	G
Mean (μm^2)	9.81247 $\times 10^2$	9.18681 $\times 10^2$	9.1363 $\times 10^2$	9.5039 $\times 10^3$	3.0322 $\times 10^3$	4.5764 $\times 10^3$	4.100 $\times 10^3$
Maximum (μm^2)	9.78243 $\times 10^3$	1.006202 $\times 10^4$	1.0402 $\times 10^4$	1.0169 $\times 10^4$	6.5845 $\times 10^4$	1.0145 $\times 10^5$	5.192 $\times 10^4$
Minimum (μm^2)	2.59000 $\times 10^2$	2.65235 $\times 10^2$	2.6673 $\times 10^2$	2.6761 $\times 10^2$	2.5810 $\times 10^2$	2.6166 $\times 10^2$	2.622 $\times 10^2$
Standard Deviation	1.24603 $\times 10^3$	1.17064 $\times 10^3$	1.1872 $\times 10^3$	1.2890 $\times 10^4$	7.7492 $\times 10^3$	1.2247 $\times 10^4$	8.580 $\times 10^3$
Whole Area (μm^2)	2.03261 $\times 10^7$	1.792345 $\times 10^7$	1.8301 4×10^7	1.8537 $\times 10^7$	1.6192 $\times 10^7$	1.4923 $\times 10^7$	1.589 $\times 10^7$
Frame Area (μm^2)	5.64116 $\times 10^7$	5.750065 $\times 10^7$	5.7922 $\times 10^7$	5.8113 $\times 10^7$	5.6052 $\times 10^7$	5.6822 $\times 10^7$	5.695 $\times 10^7$
Average Pore Area	0.361	0.311	0.316	0.319	0.289	0.262	0.279

Analytical Instruments Used to Study the Effect of Matrix Contents on the Physical Properties and Pore Structure of Spinel Refractories.

The micro-structure of each specimen was observed with a reflecting microscope (Olympas PMZ). The constituent elements and crystallization state of the specimen were analyzed qualitatively using EPMA Tracor Northern, TN-4-22 J) and X-ray diffraction (Mac Science, MXP 3), respectively.

Specimen Preparation.

1. Specimen Preparation for Pore Structure Measurement.

1.1 Chemical Composition.

Alumina beads of various sizes (0.1-1.41 mm) were used as aggregate, and alumina powder, clay, Cr_2O_3 , $\text{ZrO}_2 \cdot \text{SiO}_2$ were used as matrix additives. Table 4.3 showed the chemical composition of the raw materials. Seven specimens were prepared from different amounts of aggregates and matrices. Calcium lignosulfonate (1wt.%) was used as binder with about 1.4 - 3.0 wt. % of water. The mixture was kneaded for 15 minutes in a fret mill. After thorough kneading the mixture was pressed into compact forms of 230 x 115 x 55 mm by friction press at 0.15 mN pressure and natural dried for 16 hours, then it was further dried at 393.15 K for another 16 hours. Firing was carried out in a tunnel kiln at 2,003.15 K for 6 hours. The resulting sintered bodies were sliced into the specified sizes. Table 4.4 shows the manufacturing process of porous ceramics refractories.

ศูนย์วิทยทรัพยากร
จุฬาลงกรณ์มหาวิทยาลัย

**Table 4.3 Chemical Composition of the Aggregate and Matrix
Used for Pore Structure Measurements**

Specimen	A	B	C	D	E	F	G
Chemical Composition (wt.%)							
Aggregates	50	50					
Alumina Beads [mm] 1.0-1.41	38	20	70	65	57	40	60
Alumina Beads [mm] 0.5-1.0		18			20	30	
Alumina Beads [mm] 0.3-0.5					10	15	
Alumina Beads [mm] 0.1-0.3							
Matrices							
Alumina S 28-48 #			20	20			20
Alumina Powder A 42 [μm]	5	5	7	12	6	8	17
Clay	3.5	3.5	2	2	3.5	3.5	2
Cr ₂ O ₃	0.5	0.5	1	1	0.5	0.5	1
ZrO ₂ ·SiO ₂	3	3	-	1	-	-	1
Binder							
Calcium Lignosulfonate	(1)	(1)	(1)	(1)	(1)	(1)	(1)
Water	(2)	(2)	(1.4)	(1.5)	(3)	(3.3)	(1.7)



Table 4.4 Manufacturing Process for Porous Ceramics Refractories

Raw Materials ↓	* Alumina ball of various sizes, clay, Cr_2O_3 , $\text{ZrO}_3 \cdot \text{SiO}_2$
Mixing ↓	* Mixed for 5 minutes in fret mill
Kneading ↓	* Calcium lignosulfonate are added, then kneaded for 15 minutes in fret mill
Forming ↓	* Friction press machine at 0.15 mN produced rectangular tablets of 230 x 115 x 55 mm.
Drying ↓	* Natural drying for 16 hours * Dried at 393.15 K for 16 hours
Sintering	* Firing in tunnel kiln at 2,003.15 K for 6 hours

1.2 Characterization of Physical Properties.

Details of each physical property are described in appendix A1. They are briefly mentioned here as follows:

1. Mean Pore Size

A mercury penetration porosimeter was used to measure the pore size distribution. The pore diameter at the center of the distribution was taken as the average pore diameter.

2. Permeability

Permeability was measured according to JIS R 2215 using ambient air, and was calculated using equation (4.3). The cylindrical specimens were 50 mm in both diameter and thickness.

$$K = \frac{LQ}{A \Delta P} \quad (4.3)$$

3. Apparent Density, Bulk Density and Apparent Porosity

Porous ceramic specimens were measured for their apparent density, bulk density and apparent porosity in accordance with JIS R 2205-74. Table 4.5 summarized the physical properties of each specimen.

Table 4.5 Physical Properties of Each Specimen Used for Pore Structure Measurement

Specimen	A	B	C	D	E	F	G
Physical Properties							
Apparent Density, D_a [g/cm ³]	3.84	3.84	3.87	3.81	3.86	3.86	3.81
Bulk Density, D_b [g/m ³]	2.92	3.00	2.84	3.01	3.23	3.28	2.98
Apparent Porosity, ϵ [%]	24.1	21.7	26.6	20.85	16.4	15.0	21.4
Mean Pore Size [μm], d_e	134.6	108.2	76.8	69.70	51.2	39.20	34.0
Permeability, K [*10 ⁻⁶] [m ² /s·Pa]	3.75	2.49	0.99	0.89	0.27	0.15	0.13
Specimen Thickness, L [m]	0.009	0.009	0.005	0.005	0.003	0.003	0.005

Specimen Preparation for Studying the Effect of Matrix Contents on the Physical Properties and Pore Structure of Porous Spinel Refractories.

1. Chemical Composition.

Sintered $\text{MgO}\cdot\text{Al}_2\text{O}_3$ particles of about 0.5 to 1.0 mm in size was adopted as aggregate particles. Industrial grade rutile-type TiO_2 and sintered Al_2O_3 particles were used as additives. Table 4.6 illustrated their chemical compositions.

Five specimens were prepared from different amounts of TiO_2 and Al_2O_3 , ranging from 5 to 30 wt. % with the balance being $\text{MgO}\cdot\text{Al}_2\text{O}_3$ as aggregate. The molar ratio of TiO_2 to Al_2O_3 additive was maintained at unity. In addition, a specimen containing 10 wt. % of sintered spinel powder $\text{MgO}\cdot\text{Al}_2\text{O}_3$ as matrix and 90 wt.% $\text{MgO}\cdot\text{Al}_2\text{O}_3$ particles as aggregate was also prepared. Table 4.7 shows the weight fractions of the aggregate and matrix of all six specimens. About 3 to 7 wt. % of water was used as binder. The mixture of the aggregate and matrix was kneaded for 15 minutes in a fret mill. Subsequently, the mixture was compressed into pellets of 40 mm ϕ x 40 mm height (cylindrical form) at 98 MPa by a press machine and then dried at 393 K for 16 hours. Sintering was performed for 6 hours at 2,003.15 K in a tunnel kiln. The resulting sintered bodies were sliced into the specified sizes (0.05 m ϕ and 0.003-0.009 m thickness). Table 4.8 showed the manufacturing process of porous spinel refractories.

ศูนย์วิทยทรัพยากร
จุฬาลงกรณ์มหาวิทยาลัย

Tables 4.6 Chemical Composition of Aggregate and Matrix Used for Studying the Effect of Matrix Contents

Chemical Composition(wt.%)	Aggregate	Matrix		
	MgO·Al ₂ O ₃	TiO ₂	Al ₂ O ₃	MgO·Al ₂ O ₃
SiO ₂	0.23	0.84	0.18	0.15
TiO ₂	-	94.57	-	-
Al ₂ O ₃	72.98	3.11	99.07	72.67
Fe ₂ O ₃	0.11	0.02	0.02	0.12
CaO	0.25	0.03	0.14	0.50
MgO	26.36	0.02	0.02	26.56
Na ₂ O	0.07	0.05	0.54	-
K ₂ O	-	0.02	0.03	-
B ₂ O ₃	-	-	-	-
Ig.loss	-	1.34	-	-

ศูนย์วิทยทรัพยากร
จุฬาลงกรณ์มหาวิทยาลัย

Table 4.7 Weight Fraction of Aggregate and Matrix

Sample***	S-TA**					S-S*
	TA5	TA10	TA15	TA20	TA30	S10
Aggregate	95	90	85	80	70	90
MATRIX						
MgO·Al ₂ O ₃	-	-	-	-	-	10
TiO ₂	2.2	4.4	6.6	8.8	13.2	-
Al ₂ O ₃	2.8	5.6	8.4	11.2	16.8	-

S-TA** : Spinel titanium aluminium

S-S* : Spinel

Sample*** : By wt. %

Table 4.8 Manufacturing Process for Porous Spinel Refractories

Raw Materials ↓	* Aggregate MgO·Al ₂ O ₃ Matrix TiO ₂ , Al ₂ O ₃ , MgO·Al ₂ O ₃
Mixing ↓	* Mixed for 10 minutes in a fret mill
Kneading ↓	* Clay and binder are added, then kneaded for 10 minutes in fret mill
Forming ↓	* Compressive machine at 98 MPa produced cylindrical pellets of 40 x 40 mm.
Drying ↓	* Dried at 393.15 K for 16 hours
Sintering	* Firing in a tunnel kiln at 2,003.15 K for 6 hours

2. Characterization of Physical Properties.

Bulk density, apparent density and porosity of the specimen were measured by following JIS R2205-74. Compressive strength was measured based on JIS R2206-77. Size distribution of the pores was measured with a mercury porosimeter and volume-based on median diameter was chosen as representative pore size. Pressure drop of a specimen (40 mm in diameter and length) at various air flow rates was measured at room temperature based on JIS-R 2115. Table 4.9 showed the physical properties of the aggregate and the matrix.

Table 4.9 Physical Properties of Aggregate and Matrix Used for Studying the Effect of Matrix Contents

		Aggregate	Matrix		
		MgO·Al ₂ O ₃	TiO ₂	Al ₂ O ₃	MgO·Al ₂ O ₃
Apparent density (g/cm ³)		3.29	-	-	-
Bulk density (g/cm ³)		3.22	-	-	-
Apparent porosity (%)		2.1	-	-	-
Size (μm)	Max.	1,000	0.25	40	150
	Min.	670	0.12	5	13